JOURNAL OF AIRCRAFT
Vol. 30, No. 6, Nov.–Dec. 1993

Vortex Flow Control Using Fillets on a Double-Delta Wing

Steven B. Kern*
Naval Air Warfare Center, Warminster, Pennsylvania 18974

This article presents results from a subsonic numerical investigation on the effects of geometry modifications at the junction of the leading edge extension (LEX) and wing of a flat-plate cropped double-delta wing at moderate to high angles of attack. The baseline planform of the double-delta wing configuration consisted of a strake with a 76-deg leading-edge sweep and a wing with a 40-deg leading-edge sweep with sharp, beveled leading edges. The geometry modifications included various fillet shapes with planform areas equal to 1% of the baseline wing reference area. A hyperbolic grid generation method was developed and used in conjunction with an existing interactive grid generation system to create high quality C-O type multiblock grids about the configurations studied. The Euler and Reynolds averaged Navier-Stokes (RANS) equations were solved numerically using two finite-volume production flow solvers. The baseline configuration numerical results correlated well with existing published experimental data. Grid refinement using the RANS revealed vortex sheet tearing on the wing. Fillets enhanced the lift by 14% at low angle of attack, and 18% at high angle of attack with a slight improvement in lift-to-drag ratio. The fillets may be good candidates for roll control devices.

Nomenclature

C_D = drag coefficient
C_L = lift coefficient
C_{L0} = lift coefficient at zero angle of attack
C_M = pitching moment coefficient about the 73.27% root chord location
C_{M0} = pitching moment coefficient at zero angle of attack
c = root chord
L/D = lift-to-drag ratio
Re = Reynolds number based on root chord
X = streamwise coordinate
Y = spanwise coordinate
α = angle of attack, degrees

Introduction

MODERN fighter aircraft are designed to rely on the enhanced lift generated by vortex flow to enable high maneuverability during air-to-air combat. During carrier landing approach, vortical flows are a part of the overall flow structure of these aircraft. Current designs result in the shedding of vortices from various locations on the aircraft including the forebody, moderate to highly swept wing leading edges, strakes and leading edge extensions, and the junction of aerodynamic surfaces with each other and the fuselage. The shedding, interaction, and breakdown of these vortices are highly sensitive to both the aircraft's geometry and the flow conditions. In addition to producing the benefits of enhanced lift and maneuverability, the vortical flow also causes serious departure and structural fatigue problems.[1,2] Indeed, the ability to control the trajectory, strength, and breakdown processes of the vortices may not only alleviate the problems generated by this flow phenomena but also enhance the existing controllability, maneuverability, and agility of the aircraft.

Because of the complexity and high potential, intense research is being conducted in this field to improve the understanding of the shedding, interaction, and breakdown processes of vortex flow. This research has identified techniques for controlling vortical flow which provide additional control power, complementing conventional control surfaces. Through additional control, these techniques enhance the maneuverability and broaden the envelope of aircraft operating conditions. The goal, however, is to efficiently exploit the potential benefits of vortex flow control. Even with the developments in this field, the designer still faces trading-off additional weight and aircraft observability for enhanced performance when integrating vortex flow control concepts into an aircraft configuration.

The objective of this research is to investigate the effects of small geometry modifications (fillets) at the location of vortex shedding to control the shedding, trajectory, and subsequent breakdown of the vortex. It is believed that by affecting the shedding process at the junction of the LEX and wing, the trajectory, vortex-vortex interaction, and breakdown of the resulting vortex structure may be controlled, resulting in enhanced lift and longitudinal control. Through asymmetric deployment of the fillets, additional lateral-directional control may be created. The fillets are envisioned as being deployable at the junction of the LEX and wing. During "low observable" flight segments, the fillets would be stowed away to minimize their impact on the aircraft's observability. During air combat maneuvering or carrier landing approach, when observability is less significant, these fillets would be deployed to provide enhanced performance on demand.

Background

Recent experimental testing by Cunningham and Boer[3] confirm the vortical flow structure over a double-delta wing as described in detail by Brennenstuhl and Hummel[4] and other researchers. The planform of Cunningham's double-delta wing was identical to the double-delta wing investigated in the present study. However, the leading-edge geometry of the model in the present study was beveled to form sharp leading edges. The strake of Cunningham's double-delta wing had a leading-edge sweep of 76 deg and the wing had a leading-edge sweep of 40 deg. Cunningham's strake had sharp leading edges with a diamond-shaped lateral cross section, while the wing had rounded leading edges with NACA 64A005 longitudinal cross sections. Steady flow visualization tests at a Reynolds number of 4.2 million revealed the primary vortices originating from the strake leading edges at low angle of attack. At moderate angles of attack, vortices with the same sense of rotation as the strake vortices developed from the wing leading edges, starting at the junction of the LEX and wing as shown in Fig. 1. Also evident were secondary vortices on the upper

Presented as Paper 92-0411 at the AIAA 30th Aerospace Sciences Meeting and Exhibit, Reno, NV, Jan. 6–9, 1992; received Jan. 23, 1992; revision received Aug. 7, 1992; accepted for publication Aug. 7, 1992.

*Aerospace Engineer, Aircraft Division. Member AIAA.

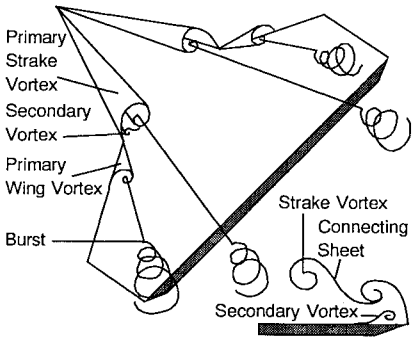

Fig. 1 Typical vortical structure over a cropped double-delta wing.

surface resulting from the spanwise separation of the upper surface boundary layer. At high angles of attack, the vortices interacted by coiling around each other. As the angle of attack was increased, vortex breakdown of the wing vortex occurred over the wing surface first, followed by the breakdown of the strake vortex.

On a double-delta wing at moderate to high angles of attack, the strake vortices and wing vortices typically begin to interact with each other as discussed in detail by Olsen and Nelson.[5] Downstream of the wing junction point, the wing and strake vortex cores coil around each other due to mutual induction. The first indication of this interaction is the simultaneous movements of the wing vortices upward and inboard, and the strake vortices downward and outboard. The strake vortices are fed vorticity from the leading edge of the strake, strengthening the vortex in the downstream direction. At the junction, the vortex sheets tear, due to the discontinuity in the slope of the sweep angle, resulting in the creation of the wing vortices. After this chordwise location, no additional vorticity is fed into the strake vortices from the leading edges of the wing. According to Kelvin's theorem, for a barotropic fluid influenced by conservative body forces, the vorticity of the particles within this vortex should only diminish by viscous dissipation. However, as suggested by Verhaagen, shear layers may exist which connect the strake vortices to the wing vortices downstream of the junction as shown in Fig. 1.[6] These shear layers would then allow vorticity to be convected from the strake vortices into the wing vortices. At higher angles of attack, either the wing or strake vortices breakdown, depending on the wing geometry. The bursting of a vortex in close proximity to an intact vortex may create enough of a perturbation in pressure to trigger the breakdown of the intact vortex.

The concept of flow control through vortex manipulation is not new. In the 1950s, H. R. Lawrence from Cornell Aeronautical Laboratories suggested the use of asymmetric edge shape effects to achieve roll control of low-aspect ratio wings at high angle of attack.[7] In the 1960s, SAAB of Sweden used closely coupled canards to delay the main wing upper surface separation on the Viggen fighter.[8] Through the 1970s the use of leading-edge extensions or strakes were developed and are now flying on the F/A-18 and F-16 aircraft. These flow control devices were primarily incorporated into the design of the aircraft to enhance lift. However, along with the desirable enhancements in lift comes undesirable stability and control problems. In 1976 Lamar hypothesized that by reducing the vortex lift on one side of a wing, and maintaining the vortex lift on the other side, a significant rolling moment could be produced.[9] Since the vortical flow dominates the lift at high angles of attack, the capability of this type of control scheme increases with angle of attack, when conventional control surfaces such as ailerons and rudders become less effective. The concept called "raked-tip" was demonstrated by changing the sweep of the cropped portion of a cropped delta wing. Since this suggestion, and because of the recent growing interest in high angle-of-attack maneuvering, substantial research is being conducted to control vortices to enhance modern aircraft maneuverability. To date, most of these vortex control methods fall into one of two categories: 1) vortex flow control through geometry modifications, and 2) vortex flow control by the transfer (suction or blowing) of secondary mass into or out of the flowfield. One similarity among all of these control concepts is that the most effective way to control vortices has been to modify the vortex at its point of origin near the shedding point at the body's leading edge. The present research involves manipulating the vortical flowfield by modifying the geometry of the wing.

Thorough reviews of vortex flow control through geometry modifications can be found in Lamar[8] and Rao.[10,11] Several methods of vortex flow management are discussed ranging from devices for enhanced lift for maneuvering and landing approach to devices for improved stability characteristics. The strake itself was originally used as a vortex flow management device, providing stable vortex systems for main wing flow separation control and enhancing lift. This prompted the idea of an articulated or hinged strake. The hinged strake is hinged longitudinally at the fuselage, allowing it to change its anhedral angle. By setting the strakes symmetrically at equal positive anhedral angles, the strake vortices are suppressed, improving the lateral-directional instabilities. Also, by setting the strakes asymmetrically, a strong rolling moment, doubling that of ailerons at high angle of attack, is achieved. Similar improvements and control can be obtained from pivotable strakes, in which the angle of attack of each strake can be modified independently.[12] Another early device called the leading-edge extension (LEE) was used on a moderately swept, thick airfoil round edge glider.[7] By attaching a sharp edge out of the leading edge radii of the glider's wing, a vortex was created and captured at the leading edge. This vortex created suction on the leading edge, resulting in forward thrust to reduce the drag at the higher lift conditions. A similar and effective concept is vortex flaps. Leading-edge flaps or vortex flaps were originally developed to reduce drag during transonic maneuvering. However, vortex flaps, and variations of the concept, including apex flaps and fences, are capable of providing enhancements in lift and longitudinal stability as well. Several concepts have been used to effectively break up the large primary vortex systems. These concepts fall under the category of compartmented leading edges and are similar to the concept of using fillets on a double-delta wing. The methods of compartmenting the leading edges include fences, slots, and pylon vortex generators. These devices cause the primary vortex to break up into several vortices by tearing the vortex sheet and creating counter-rotating vortices. They result in a drag reduction and improved longitudinal stability. A more detailed background on vortex flows may be found in Ref. 13.

Approach

This study focused on the ability of geometry modifications that may be potentially applied to existing or future high-performance aircraft. For this reason, it was important that the baseline configuration resembled a fighter such that any promising concept could be extended to a realistic configuration. However, due to the complexity and therefore, the large computational requirements of modeling the forebody, fuselage and tails of a full configuration, only the LEX and wing was analyzed. Moreover, the simplified LEX-wing combination analyzed isolates the basic vortex flow structure to be controlled, without the additional complications of forebody vortex, fuselage, and tail interactions.

A comparison of LEX-wing planform shapes ranging from research oriented studies to actual configurations is presented in Fig. 2. Each of these configurations has a LEX which extends about 50% of the chord whose leading-edge sweep is within 76 and 80 deg. In contrast to the high sweep of typical double-delta wings, the leading-edge sweep of the wings of the F/A-18 and YF-23 are about 26 and 40 deg. Also shown

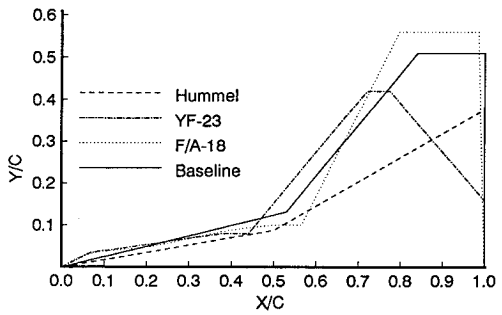

Fig. 2 Planform comparison.

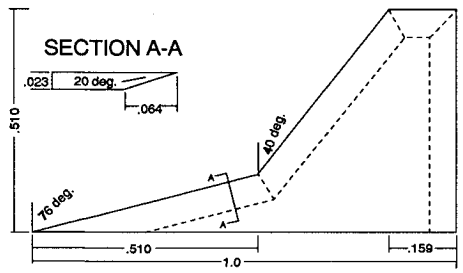

Fig. 3 Model dimensions.

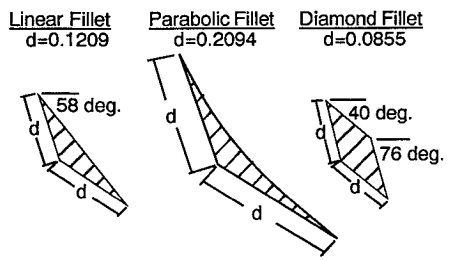

Fig. 4 Fillet dimensions.

is the cropped double-delta wing recently tested by Cunningham in an unsteady experimental study.[3] Because of its resemblance to modern aircraft in planform and the extensive experimental data base that exists, this configuration was chosen as the baseline.

To simplify the fabrication of an experimental model, a beveled leading-edge flat-plate version of Cunningham's model was chosen for the future experimental studies and was subsequently employed for the current computational analysis. The model geometry used in all simulations in the present work is shown in Fig. 3.

To control the vortex flow, three fillet shapes were included at the junction of the LEX and wing of the baseline configuration. The planform area of the fillets analyzed were 1% of the wing reference area and are shown in Fig. 4. The basic fillet shapes investigated were 1) linear fillets; 2) smooth parabolic fillets whose slope matched the LEX and wing slopes at their intersection, respectively; and 3) diamond-shape fillets. The upper surface of the fillets were flat and coplaner with the wing upper surface. The lower surface of the fillets were constructed by fairing the geometry of the leading edge of each fillet to the beginning of the bevel on the lower surface of the baseline wing. The parabolically shaped fillets removed the discontinuity in slope at the junction, while the linear and diamond-shaped fillets added additional discontinuities in this region at which vortices were expected to originate.

The numerical approach was to use the Euler equations extensively followed by correlation with RANS simulation. During the course of investigations several grids having different numbers of grid points and grid point clustering were used. Aerodynamic coefficients of the baseline configuration were correlated with Cunningham's steady-state results.

Grid Generation

A three-dimensional hyperbolic grid generation method was developed for use in conjunction with an existing interactive grid generation system to create high-quality spherical C-O topology multiblock grids. Several requirements were met in the generation of grids over the double-delta wing including 1) the use of a C-O topology; 2) field grid clustering in the normal direction at the surface of the wing to resolve the boundary layer flow in the viscous simulations; 3) surface grid clustering at the apex, along the leading edges, and at the trailing edge of the wing; 4) a high level of field grid orthogonality; 5) a multiblock grid approach to minimize computer core memory requirements; and 6) sufficient field grid density in the regions of rotational flow to resolve the vortices.

The surface geometry and surface grid were generated by using the zonal interactive graphics for grid generation (ZI3G) module of the graphically interactive McDonnell aircraft computational grid system (MACGS). The coarse surface grid had 66 points in the chordwise direction and 73 points in the circumferential direction. The fine surface grid had 66 points in the chordwise direction and 101 points in the circumferential direction. For the fine grid, 65 of the circumferential points were clustered on the upper surface. The leading edges of the strake and wing were made sharp to force separation along one grid line. The geometry of the surface grid leading edges was used for both inviscid and viscous analyses and is shown in Fig. 5. The surface grid was clustered at the apex, the leading edges, and the trailing edge by using hyperbolic tangent distributions.

Several field grids were generated and are detailed in Table 1. For all field grids, the far-field boundary was within 2–2.5 chord lengths away from the body in all directions. The fine grid was split into an inner rotational and an outer irrotational zone. The inner zone extended away from the wing 0.6 chord lengths. Based on previous single delta wing simulations, all

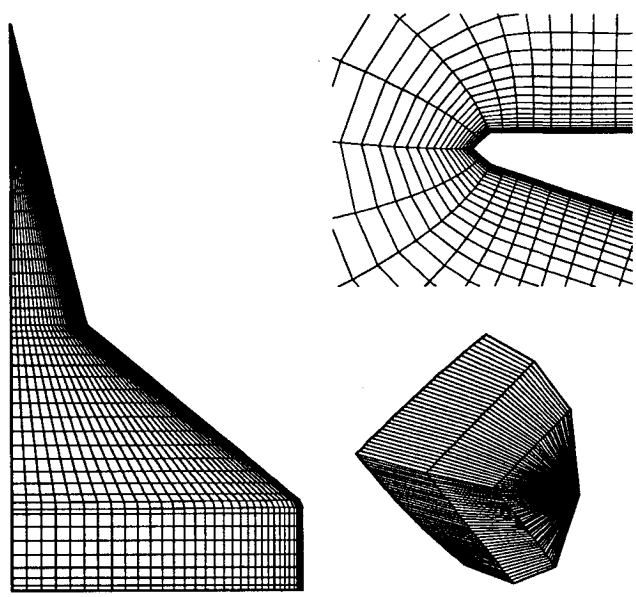

Fig. 5 Surface grid.

Table 1 Grid dimensions

Grid no.	Dimensions	Zone	Boundary layer type	Total points
1	81 × 73 × 53	Single	Inviscid	313,389
2	81 × 55 × 71	Upper	Viscous	425,574
	81 × 19 × 71	Lower		
3	81 × 77 × 55	Upper inner	Viscous	554,931
	81 × 25 × 55	Lower inner		
	81 × 73 × 17	Outer		

of the rotational flow has been within 0.6 chord lengths of the wing. The surface was used as the initial condition for the hyperbolic grid generation method to create the field grids. The field grid was generated by marching in the direction normal to the wing. This method used two orthogonality conditions and a geometric constraint, and was based on the development by Steger and Rizk[14] which was extended by Chan and Steger.[15] The resulting system of partial differential equations were hyperbolic in nature, and methods similar to those used in solving the Euler equations were used. The hyperbolic system was solved by using an approximate-factored, noniterative, implicit, finite difference scheme with adaptive dissipation to filter odd-even decoupling and enhance the robustness of the scheme at sharp corners. The normal grid cell clustering was achieved by specifying the cell volumes at each iteration in space. The spacing in the normal direction was controlled such that for the viscous grids 17–21 grid cells fell within the boundary layer. The process of generating a high-quality, positive cell volume grids was iterative because of the sensitivity of the hyperbolic system to the initial conditions (the surface). Several surface grids were generated before acceptable field grids were obtained.

Computational Method

Two production flow solvers were used in this analysis. The three-dimensional Euler/Navier-Stokes aerodynamic method (TEAM) code was used to solve for the inviscid rotational flow over the double-delta wings.[16] The code applies a cell-centered finite volume scheme to discretize the spatial terms modified by second- and fourth-order adaptive numerical dissipation. The scheme has an option for a second-order space accurate, upwind, Roe flux-differencing method. The equations are integrated in time explicitly by using a multistage Runge-Kutta algorithm which employs enthalpy damping, implicit residual smoothing, and pseudotime marching to accelerate convergence to steady state.

For viscous analyses, the Navier-Stokes time dependent (NASTD) flow solver developed by McDonnell Aircraft Co. was used.[17] The code implements a finite volume domain decomposition to maximize the robustness in regions having skewed grids. The solver uses an implicit Beam and Warming-type approximate-factored scheme.[18] The code also has the option of using an upwind formulation with additional terms being added to implement total variation diminishing (TVD) to increase the accuracy of the scheme to second order in regions where the solution is smooth. The TVD formulation used attempts to insure the physical modeling of discontinuities in the flowfield such as shocks and contact discontinuities which include shear layers. Both TEAM and NASTD have been previously validated for subsonic vortical flows.[16,19–21]

Discussion of Results

The flow over the baseline wing without fillets was investigated first by employing the three grids using both TEAM and NASTD. TEAM was run at Mach 0.3 using grid no. 1 at angles of attack of 0, 10, 16, 19, 22.5, and 27.4 deg. NASTD was run at Mach 0.2 at a Reynolds number of 1 million based on root chord for all three grids at an angle of attack of 22.5 deg exclusively. All viscous simulations employed the Baldwin-Lomax algebraic turbulence model over the entire wing surface. The viscous flow over grid no. 3 was solved at Reynolds numbers of both 1 and 4 million.

The average residuals (L2 norm) of all inviscid simulations using TEAM were reduced by four orders of magnitude, requiring between 1000–2000 iterations for convergence. A cell-based CFL number of 6 was used with implicit residual smoothing and pseudotime marching to accelerate convergence to steady state. Fourth-order adaptive dissipation was used to filter the odd-even decoupling. Second-order dissipation was kept at a minimum because no shocks were expected to form at the low speeds investigated.

When using NASTD for the viscous simulations, the TVD option was invoked. The residuals in NASTD were reduced by 2.5 orders of magnitude to reach steady-state convergence, which required 1500–2000 iterations. A cell-based Courant-Friedrichs-Lévy (CFL) number of 1.3 was used with pseudotime marching and for the first 500 iterations grid sequencing was used to accelerate convergence to steady state.

Baseline Inviscid Analysis

At an angle of attack of 10 deg, two well defined vortices developed from the leading edges of the LEX and wing, respectively, as shown in Fig. 6a. The LEX and wing vortices were convected downstream over the leeward surface of the double-delta wing without any interaction. The LEX vortex was nearly conical over the LEX portion of the wing. Both vortices induced spanwise velocity on the wing surface, resulting in a local increase in suction beneath each vortex core (not shown). The suction beneath the wing vortex, especially at the junction, was higher than the suction developed beneath the LEX vortex. This indicates that the wing vortex was stronger than the LEX vortex. According to Hemsch and Luckring,[22] the strength of a vortex increases with decreasing sweep, which is consistent with the present findings.

At an angle of attack of 16 deg, the LEX and wing vortices interacted with each other as shown in Fig. 6b. With an increase in angle of attack, the mutual influence of the vortices increased. The LEX vortex induced an upward and inboard movement of the wing vortex. Conversely, the wing vortex induced a downward and outboard movement of the LEX vortex. The interaction of the two vortices caused them to intertwine upstream of the trailing edge of the double-delta wing. As the angle of attack was increased to 19 deg, the vortices strengthened. This amplified their mutual influence, and caused them to intertwine slightly farther upstream of the trailing edge of the double-delta wing than at 16 deg.

At an angle of attack of 22.5 deg, the vortices intertwined farther upstream than at 19 deg and merged into one vortex core. The individual cores of the LEX and wing vortices downstream of the point of interaction could no longer be distinguished due to the lack of grid resolution in the vicinity of the cores. As the angle of attack was increased to 22.5 deg, the flow in the cores of the vortices nearly stagnated before the trailing edge, indicating the onset of vortex breakdown. At an angle of attack of 27.5 deg (not shown) the code did not converge. By observing the unconverged solutions at different pseudotime steps, the flow was found to be unsteady due to fluctuations in the position of vortex breakdown. Since pseudotime marching was employed in this TEAM simulation, the unconverged results at 27.4 deg angle of attack were meaningless, and are not presented.

Baseline Viscous Analysis

To obtain a comparison with the inviscid flow, grid no. 1 was initially run using NASTD. Particle traces beginning at the leading edge at an angle of attack of 22.5 deg for the inviscid and viscous analyses are shown in Fig. 7 for direct comparison. This plot shows good correlation of the structure and interaction of the primary LEX and wing vortices. By investigating the flow near the surface, it was determined that less than 10 grid points normal to the surface were included in the boundary layers on the double-delta wing in the viscous analysis. Because of the lack of clustering near the surface, the viscous analysis did not resolve the spanwise boundary-layer separation and the subsequent roll-up of secondary vortices. Two additional grids were run to improve on this result. In both grids nos. 2 and 3, 17–21 grid points were clustered normal to the surface in the boundary layer. Particle traces of these viscous simulations are shown in Figs. 7c and 7d.

The locations of the LEX and wing vortices correlated well between all the grids, but the structure of the wing vortex for grid no. 3 was unusual. Midway down the leading edge of the wing on the viscous simulation of grid no. 3, a second wing

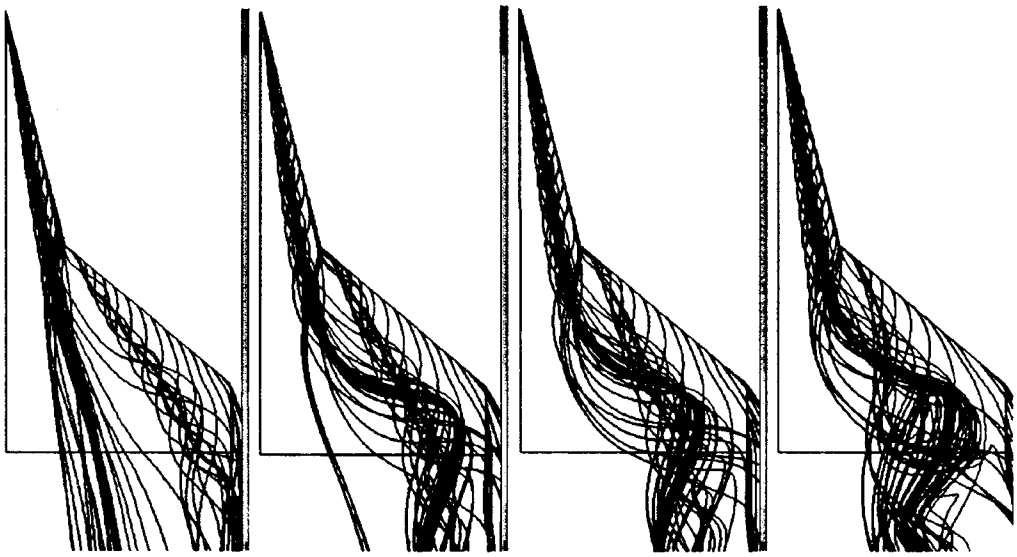

a) α = 10 deg b) α = 16 deg c) α = 19 deg d) α = 22.5 deg

Fig. 6 Effect of angle of attack on the baseline wing inviscid vortex flow particle traces.

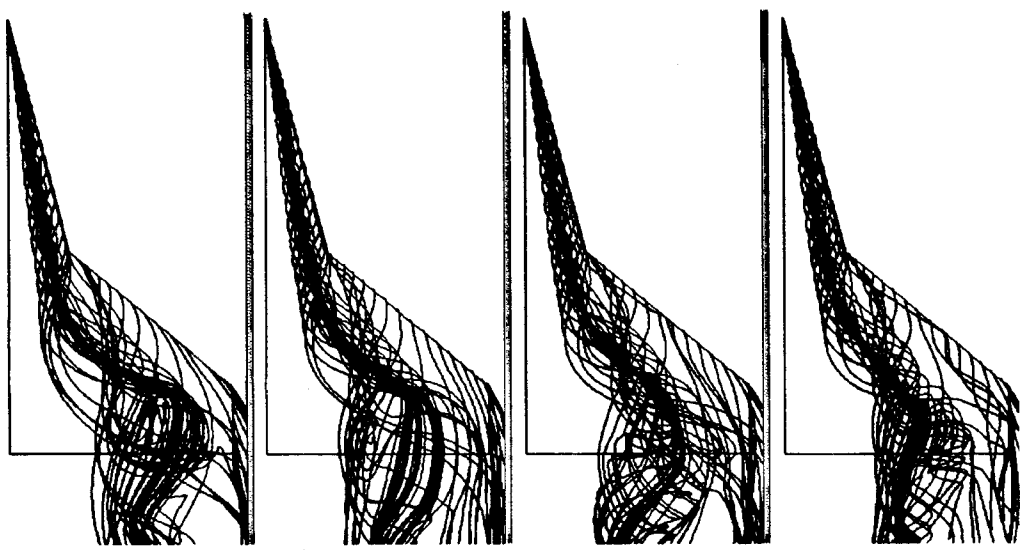

a) Inviscid-grid no. 1 b) Viscous-grid no. 1 c) Viscous-grid no. 2 d) Viscous-grid no. 3

Fig. 7 Effect of viscosity and grid resolution on the baseline vortex flow particle traces at α = 22.5 deg.

vortex appeared. This phenomena called "vortex tearing" has usually not been produced in numerical investigations but has been seen in experimental tests performed on double-delta wings that have moderately swept wing leading edges.[23-25] The tearing of the wing vortex is caused by the interaction of the LEX and wing vortices. Since the wing vortex is drawn away from the wing leading edge by the LEX vortex, the distance the connecting shear layer must extend to reach the core of the wing vortex increases. As this distance is increased, it becomes increasingly more difficult for the shear layer to remain smooth because of the inherent instability of free shear layers. It is believed that the shear layer's instability causes the shear layer to roll-up upon itself and create the additional torn wing vortex. An extension of Verhaagen's connecting sheet concept in Fig. 1 can be applied to this phenomena.[6] A chordwise cross section of the proposed new vortex structure with connecting shear layers is shown in Fig. 8.

Based on a survey of the literature, vortex tearing has not been produced on experimental tests of 80/60-deg double-delta wings. Therefore, it is believed that the particular combination of parameters including the moderate LEX sweep, the moderate wing sweep, and the flow conditions of this investigation contributes to the formation of a torn primary

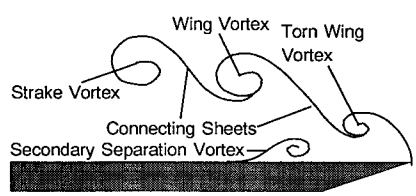

Fig. 8 Proposed double-delta wing vortex shear layer cross section with a torn wing vortex.

wing vortex. Since the sweep of the LEX of an 80/60-deg double-delta wing is larger than the sweep of the present LEX, the LEX vortex of the present wing is stronger than the LEX vortex on an 80/60-deg double-delta wing. Since the LEX vortex of the present wing is stronger, it easily draws the wing vortex upward and inboard. The combination of the large inboard movement of the wing vortex and the wing's modest sweep results in the tearing on the present configuration.

To investigate the effect of Reynolds number, NASTD was used to solve for the viscous flow over grid no. 3 at a Reynolds number of 4 million. This simulation showed little difference in the structure of the primary leading-edge vortices, the lo-

cation of vortex intertwining, or the generation of a torn wing vortex when compared to the solution at a Reynolds number of 1 million.

Correlation with Experiment

The aerodynamic coefficients of the baseline double-delta wing from the numerical simulations were correlated with the experimental steady-state data from Cunningham.[3] In order to make a proper comparison, the lift curves for both the experimental and the present study were shifted by the lift at zero angle of attack. The resulting lift coefficients are shown in Fig. 9. The drag polar was similarly shifted by the lift at zero angle of attack and is shown in Fig. 9. The pitching moment about the 73.27% chord point was shifted by the pitching moment at zero angle of attack and is also shown in Fig. 9.

The inviscid simulations showed good correlation with experimental lift, drag, and pitching moment for the range of angles of attack investigated. The viscous simulations had good correlation in lift and drag, and fair correlation in pitching moment at 22.5 deg angle of attack. The discrepancy in pitching moment is attributed to the differences in edge shape of the experimental and the present models.

Effect of Fillets

As shown in the previous section, the vortical flowfield that exists over the baseline wing can be quite complex, containing primary vortices from the LEX and wing and secondary vortices due to boundary-layer separation, and even torn wing leading-edge vortices. The focus of this research, however, was to determine the effects on the primary vortex structure and aerodynamics of adding fillets to the baseline wing at the junction. Since the Euler equations were capable of predicting the primary vortical structure on the baseline wing, and the aerodynamic coefficients correlated well with the experiment, they were used to determine the effect of the fillets.

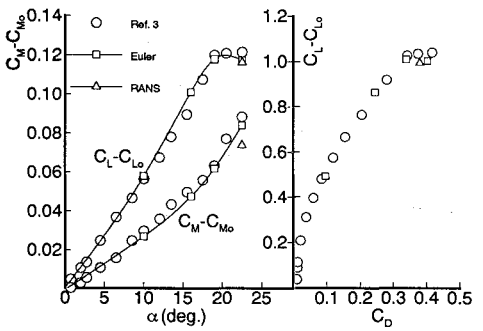

Fig. 9 Correlation of longitudinal aerodynamic coefficients with experiment.

The surface geometry was modified to include the three fillet shapes and used to generate corresponding field grids. To minimize grid-dependent solutions, the number of grid points and grid clustering for the fillet grids was kept identical (except near the region of the fillets) to the baseline double-delta wing grid no. 1. The new fillet grids were run using TEAM exclusively at Mach 0.3 at angles of attack of 0, 10, 16, 19, 22.5, and 27.4 deg.

An angle of 10 deg is within the angle-of-attack range of Naval fighters approaching a carrier for landing. The particle traces of the new primary vortex cores along with the baseline are shown in Fig. 10. By removing the sharp discontinuity at the junction of the wing, the parabolic fillet combined the LEX and wing vortex feeding sheets into one single feeding sheet along the entire length of the leading edge from the apex to the cropped portion. This single sheet rolled up into one large vortical structure over the leeward side of the wing. The position of this vortex was far outboard of the original LEX primary vortex system. In fact, the trajectory of the single vortex system came very close to the baseline primary wing vortex towards the trailing edge of the wing.

The linear fillet caused the vortex feeding sheet to tear at the junction of the fillet and the LEX. The resulting sheet generated an additional vortex from the fillet which intertwined with the LEX vortex just downstream of the midchord point, forming a single vortex core due to the lack of grid resolution in the vicinity of the cores. The resulting joined LEX/fillet vortex then intertwined with the wing vortex near the trailing edge of the wing.

The diamond-shape fillet also caused the sheet to tear at the junction of the fillet and LEX. The resulting sheet generated an additional vortex feeding sheet which rolled up into a single fillet vortex. This vortex also intertwined with the LEX vortex just downstream of the midchord point. The point of interaction of the LEX-fillet vortex of the diamond fillet was upstream of the point of interaction of the linear fillet LEX-fillet vortex.

At this low angle of attack of 10 deg, all of the fillets moved the entire primary vortex system outboard. The corresponding suction on the surface of the wing due to the vortical flow was shifted outboard as well. Further investigation is required to determine the enhancements in rolling moment due to this shift in moment arm caused by the fillets.

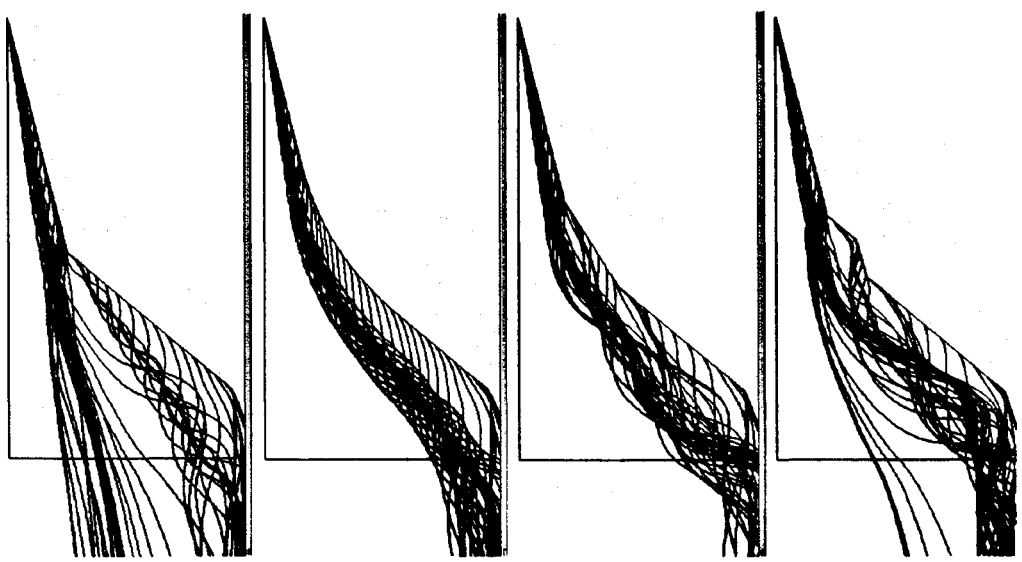

a) Baseline b) Parabolic c) Linear d) Diamond

Fig. 10 Effect of 1% area fillets on the inviscid vortex flow particle traces at α = 10 deg.

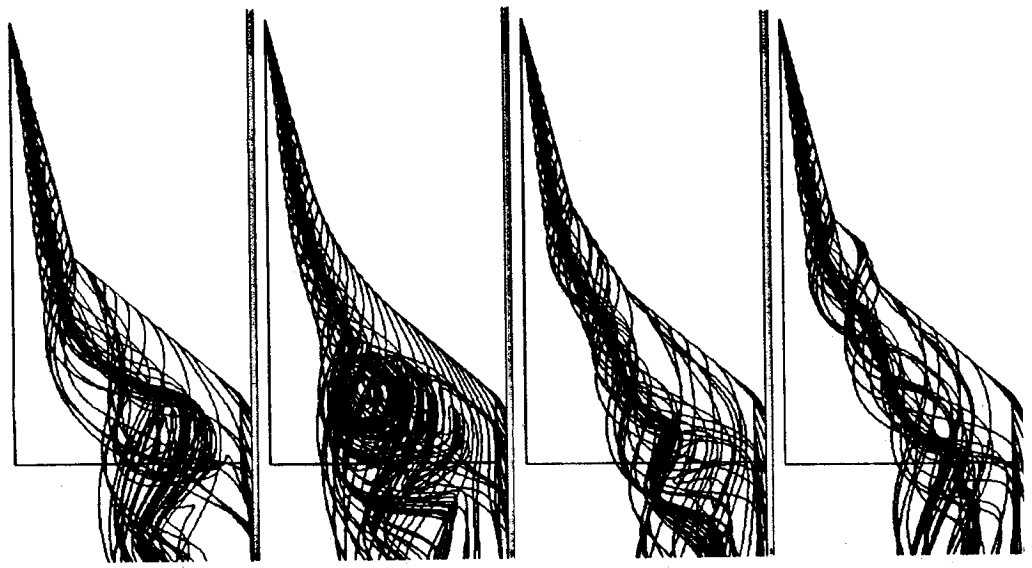

a) Baseline b) Parabolic c) Linear d) Diamond

Fig. 11 Effect of 1% area fillets on the inviscid vortex flow particle traces at α = 22.5 deg.

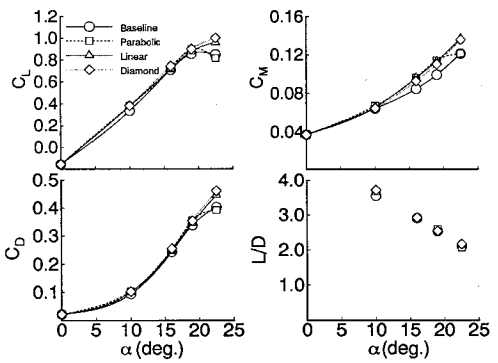

Fig. 12 Effect of 1% area fillets on the longitudinal aerodynamics of the baseline cropped double-delta wing.

At an angle of attack of 22.5 deg, which is representative of the angle of attack at which current Naval fighters maneuver, the fillets created similar vortex structures to those at 10 deg as shown in the particle traces in Fig. 11. However, the controlled primary vortices were not drawn as far outboard than at the lower angle of attack. The parabolic fillet combined the LEX and wing vortex feeding sheets. The vorticity in the feeding sheet becomes stronger as the sweep of the wing decreases through the region of the fillet and the wing. Therefore, since all of the vorticity from the entire leading edge of the LEX and wing entered the vortex, the vortex was more apt to breakdown farther upstream. The linear fillet generated a vortex that intertwined around the LEX vortex. The major effect of the linear fillet was to separate the LEX vortex from the wing vortex. By separating these vortices, a favorable effect of interaction between the LEX and wing vortices was created, which delayed vortex breakdown. Similar effects were found with the diamond-shape vortex. However, the onset of vortex breakdown with the diamond fillet was postponed farther downstream than the linear fillet.

The longitudinal aerodynamic characteristics of the fillets compared with the baseline are plotted in Fig. 12. At a low angle of attack of 10 deg, the parabolic, linear, and diamond-shaped fillets enhanced the lift by 13, 13, and, 14%, respectively. At a high angle of attack of 22.5 deg, the parabolic fillet degraded the lift by 4.0% due to premature breakdown. The linear fillet and diamond fillet enhanced the lift by 13 and 18%, respectively, by delaying the onset of breakdown and providing additional suction near the junction of the double-delta wing due to the increase vortex strength in that region. There was a corresponding drag penalty for more lift, but the *L/D* ratio was basically unaltered as a result of the fillets as shown in Fig. 12. In fact, at the lower angle of attack of 10 deg, the *L/D* ratio improved slightly. Along with the increase in lift comes a pitch-up moment. This pitch-up is believed to be associated with the additional lift generated near the junction of the wing due to the presence of the fillets.

Conclusions

This investigation has shown that small deployable fillets at the junction of a double-delta wing provide substantial control over the downstream vortical trajectory and breakdown locations. By increasing the grid resolution, the numerical simulations revealed the process of vortex sheet tearing. This study suggests that the tearing is a result of the interaction of the LEX and wing vortices, especially the inboard displacement of the wing vortex. No apparent Reynolds number effects on the tearing process were found. Further grid resolution in inviscid simulations is required to determine if the tearing process is dependent on the presence of viscosity. At low angle of attack, all fillets shifted the vortex structure outboard. This type of control may lead to enhanced roll control or a method of alleviating tail buffet by deflecting the vortex away from the empennage surfaces at certain angles of attack. The shift in upper surface suction caused by the fillets must be investigated further to determine its impact on rolling moment. At the higher angle of attack, the fillets delayed vortex breakdown by providing a favorable vortex interaction. The delay in breakdown provided up to 18% lift enhancement with a slight improvement in *L/D* ratio.

Acknowledgments

The author would like to thank the following people: Marvin Walters, David Findlay, Wei Tseng, Hugo Gonzalez, and Sam Greenhalgh for their encouragement and technical support at NADC; Bob Bush, Bill Romer, and Walt LaBozetta for help using MACGS and NASTD at McDonnell Aircraft Co.; Lyle N. Long for advice using TEAM at the Pennsylvania State University; and James Luckring, Gary Erickson, William Straka, and Neal Frink for their discussions and encouragement at NASA Langley Research Center.

References

[1]Shah, G. H., Grafton, S. B., Guynn, M. D., Brandon, J. M., Dansberry, B. E., and Patel, S. R., "Effect of Vortex Flow Characteristics on Tail Buffet and High-Angle-of-Attack Aerodynamics

of a Twin-Tail Fighter Configuration," *High-Angle-of-Attack Technology Conference*, NASA LaRC, NASA CP 3149, Nov. 1990, pp. 1087–1148.

[2]Lan, E. C., and Lee, I. G., "Investigation of Empennage Buffeting," NASA CR-179426, Jan. 1987.

[3]Cunningham, A. M., Jr., and den Boer, R. G., "Unsteady Low Speed Windtunnel Test of a Straked Delta Wing, Oscillating in Pitch," Air Force Wright Aeronautical Lab. TR-87-3098, Pts. I–VI, Wright-Patterson AFB, OH, April 1987.

[4]Brennenstuhl, U., and Hummel, D., "Vortex Formation over Double-Delta Wings," International Council of the Aeronautical Sciences 82-6.6.3, Germany, 1982.

[5]Olsen, P. E., and Nelson, R. C., "Vortex Interaction over Double-Delta Wings at High Angle of Attack," AIAA Paper 89-2191-CP, 1989.

[6]Verhaagen, N. G., "An Experimental Investigation of the Vortex Flow over Delta and Double-Delta Wings at Low Speed," Delft Univ. of Technology, Rept. LR-372, The Netherlands, Sept. 1983.

[7]Barlett, G. E., and Vidal, R. J., "Experimental Investigation of Influence of Edge Shape on the Aerodynamic Characteristics of Low Aspect Ratio Wings at Low Speeds"' *Journal of the Aeronautical Sciences*, Vol. 22, No. 8, 1955, pp. 517, 534.

[8]Lamar, J. E., "Nonlinear Lift Control at High Speed and High Angle of Attack Using Vortex Flow Technology," AGARD, 1986, pp. 4-1, 4-21.

[9]Lamar, J. E., "Prediction of Vortex Flow Characteristics of Wings at Subsonic and Supersonic Speeds," *Journal of Aircraft*, Vol. 13, No. 7, 1976, pp. 490, 494.

[10]Rao, D. M., "Vortical Flow Management for Improved Configuration Aerodynamics—Recent Experiences," AGARD Symposium on Aerodynamics of Vortical Type Flows in Three Dimensions, AGARD CP-342, Paper 30, Rotterdam, The Netherlands, April 1983.

[11]Rao, D. M., and Campbell, J. F., "Vortical Flow Management Techniques," *Progress in Aerospace Sciences*, Vol. 24, 1987, pp. 173–224.

[12]Bobbitt, P. J., and Foughner, J. T., "Pivotable Strakes for High Angle of Attack Control," Society of Automotive Engineers Paper 851821, Oct. 1985.

[13]Kern, S. B., "Investigation of Vortex Flow Control, Using Fillets at the Strake/Wing Junction of a Double-Delta Wing," M.S. Thesis, Pennsylvania State Univ., University Park, PA, 1992.

[14]Steger, J. L., and Rizk, Y. M., "Generation of Three-Dimensional Body Fitted Coordinates Using Hyperbolic Partial Differential Equations," NASA-TM-86753, June 1985.

[15]Chan, W. M., and Steger, J. L., "A Generalized Scheme for Three-Dimensional Hyperbolic Grid Generation," AIAA Paper 91-1588-CP, June 1991.

[16]Raj, P., et. al., "Three-Dimensional Euler/Navier-Stokes Aerodynamic Method," Air Force Wright Aeronautical Lab. TR-87–3074, Vols. I–III, Wright-Patterson AFB, OH, June 1989.

[17]Bush, R. H., "A Three Dimensional Zonal Navier-Stokes Code for the Subsonic Through Hypersonic Propulsion Flowfields," AIAA/SAE/ASME 24th Joint Propulsion Conf., July 11–13, 1988.

[18]Beam, R., and Warming, R. F., "Implicit Finite Difference Algorithm for Hyperbolic Systems in Conservation Law Form," *Journal of Computational Physics*, Vol. 22, Sept. 1976, pp. 87–110.

[19]Raj, P., Keen, J. M., and Singer, S. W., "Applications of an Euler Aerodynamics Method to Free-Vortex Flow Simulation," AIAA Paper 88-2517-CP, 1988.

[20]Tseng, W., and Findlay, D. B., "Analysis of Viscous Flowfield Over Tactical Aircraft Forebody and Inlets," American Society of Mechanical Engineers Paper 90-GT-387, June 1990.

[21]Findlay, D. B., and Kern, S. B., "Numerical Investigation of the Effect of Blowing on High Angle of Attack Flow over Delta Wings," AIAA Paper 91-1809, June 1991.

[22]Hemsch, M. J., and Luckring, J. M., "Connection Between Leading-Edge Sweep, Vortex Lift, and Vortex Strength for Delta Wings," *Journal of Aircraft*, Vol. 27, No. 5, 1990, pp. 473–475.

[23]Squire, L. C., Jones, J. G., and Stanbrook, A., "An Experimental Investigation of the Characteristics of some Plane and Cambered 65 Degree Delta Wings at Mach Numbers from 0.7 to 2.0," R&M 3305, UK, 1963.

[24]Erickson, G. E., "Wind Tunnel Investigation of Vortex Flows on F/A-18 at Subsonic Through Transonic Speeds," NASA TP 3111, Dec. 1991.

[25]Erickson, G. E., "Wind Tunnel Study of the Interaction Breakdown Characteristics of Slender Wing Vortices at Subsonic, Transonic, and Supersonic Speeds," NASA TP-3114, Nov. 1991.